EASR

Engineering and Applied Science Research

https://www.tci-thaijo.org/index.php/easr/index

Published by the Faculty of Engineering, Khon Kaen University, Thailand

Removal of cationic dye from textile wastewater using treated bagasse fly ash: An industrial waste

Areeya Chumpiboon[1)], Kananan Thongsubsai[1)], Thanatporn Pongsiri[1)], Jesper T.N. Knijnenburg[2)] and Yuvarat Ngernyen*[1)]

[1)]Biomass & Bioenergy Research Laboratory, Department of Chemical Engineering, Faculty of Engineering University, Khon Kaen 40002, Thailand
[2)]Biodiversity and Environmental Management Division, International College, Khon Kaen University, Khon Kaen 40002, Thailand

Received 11 July 2021
Revised 5 September 2021
Accepted 15 September 2021

Abstract

This study examines the treatment of bagasse fly ash (BFA), a solid waste generated from boilers in the sugar industry, using acid (HCl, H_2SO_4 and HNO_3) treatment and carbonization under N_2 atmosphere. The obtained adsorbents were characterized for their porous properties including BET surface area, total pore volume and average pore size. The treated fly ash with the highest surface area (TFA) was studied in detail for its physicochemical properties and the adsorption of methylene blue (MB) dye from aqueous solutions, and was compared with untreated BFA and a commercial activated carbon (CAC). The physicochemical characterization indicated that BFA and TFA represent adsorbents with low and moderate surface area (26 and 239 m^2/g, respectively) with functional groups on their surface, while CAC has a high surface area (1130 m^2/g) with weak surface functional groups. For all three adsorbents, the MB adsorption equilibrium was attained within 90 min and the kinetic data were best described by pseudo-second order and intra-particle diffusion kinetic models. The adsorption isotherms followed the Langmuir equation with a maximum MB adsorption capacity of 27.2, 39.0 and 42.1 mg/g for BFA, TFA and CAC, respectively. The comparable adsorption capacities of TFA and CAC suggest that the MB adsorption involves both surface area and surface functional groups on the adsorbents. Thus, this study demonstrates that BFA, a low cost solid waste, can be converted by simple treatment into an effective adsorbent for MB removal from aqueous solution with performance comparable to that of high surface area CAC.

Keywords: Bagasse fly ash, Treated fly ash, Adsorption, Methylene blue, Isotherm

1. Introduction

Methylene blue (MB) is a basic (cationic) dye that is frequently used for dyeing cotton, silk and wood in the leather, paper, textiles, rubber, plastics, printing, cosmetics, pharmaceutical and food industries [1, 2]. MB can cause permanent injury to the eyes, increased heart rate, nausea, vomiting, shock, mental confusion, cyanosis, jaundice and quadriplegia [1, 3, 4]. Thus, it is important to remove this dye from discharged wastewater due to its toxicological and aesthetic impact on receiving waters.

In recent years, various studies have been done on the removal of MB from aqueous solutions by several methods. Examples include the use of membranes [5, 6], nanobiocatalysts [7], chemical oxidation using a Fenton-like reaction [8], biodegradation [9], combined adsorption and photodegradation [10], liquid-liquid extraction [11], electrocoagulation [12], and adsorption by various adsorbents such as activated carbon [13], synthesized alumina-zirconia composite [14] or nickel alginate/graphene oxide aerogel [15]. Of these techniques, adsorption is generally preferred because of its simple design, easy operation, low cost, abundant choice of adsorbent materials, relatively simple regeneration and high efficiency [4, 5]. Activated carbon is one of the most commonly used adsorbents due to its high specific surface area and adsorption capacity, but it suffers from high production and regeneration cost [3, 16]. This limits its use and thus necessitates the development of low-cost adsorbents. As an alternative, carbonaceous agricultural, municipal and industrial wastes have been converted into low-cost porous materials for dye removal [17].

Fly ash is a waste that is generated in large volumes by many industries, such as the combustion of coal or agricultural by-products in electric utility or industrial boilers. Sugarcane is an important economic crop in Thailand for sugar production. The by-product, bagasse, has a high calorific value and is hence utilized as a fuel for boilers in sugar mills to generate steam and electricity. The efficiency of such boilers used in sugar mills is 60-70% [18], thus the burning of bagasse results in the generation of fly ash due to incomplete carbonization of the sugarcane bagasse. This fly ash has a considerable content of unburned carbon and can potentially be used as an effective adsorbent.

The utilization of fly ash as adsorbent for dye removal from wastewater could be economically attractive. However, the as-received fly ash has a low adsorption capacity. Wang et al. [19] used five types of coal fly ash and the maximum MB adsorption capacity was only 7 mg/g. Khan et al. [20] utilized fly ash from a thermal power station for the removal of MB and the maximum monolayer adsorption capacities were 2.69-4.28 mg/g. Nevertheless, the adsorption capacity of fly ash can be increased by modification using

*Corresponding author.
Email address: nyuvarat@kku.ac.th
doi: 10.14456/easr.2022.39

physical and/or chemical methods. For example, Li et al. [21] used high-energy ball milling to modify coal fly ash. Freitas et al. [22] used CO_2 to activate bagasse fly ash at 800 °C for 2 h. Shah et al. [23] modified sugarcane bagasse fly ash by chemical treatment with 3 M NaOH and 3M NaOH+1.5 M NaCl solution at 100 °C for 72 h. Additionally, acid treatments such as 1 M H_2SO_4 at 50 °C for 24 h [24], 20% HCl, 20% H_2SO_4 and mixed HCl and H_2SO_4 [25] and 1 M HNO_3 for 24 h [26] have also been used. Wang et al. [27] treated fly ash with 1 M HCl at room temperature and 100 °C for 24 h. They also treated fly ash with HCl solution in an ultrasonic bath for 1 h, as well as under microwave heating for 2 and 10 min. Fly ash has also been used as raw material to produce activated carbon. Purnomo et al. [28] produced bagasse fly ash based activated carbon by $ZnCl_2$ activation and $ZnCl_2$ simultaneous with CO_2 activation. In this process, the bagasse fly ash was first treated with concentrated $ZnCl_2$ and subsequently carbonized or activated with N_2 or CO_2 at 500-700 °C for 1 h. The KOH activation of fly ash followed by heating under N_2 was also performed for preparation of activated carbon [29, 30]. Very recently, researches have mixed fly ash with other materials to produce activated carbons, such as coconut shell with coal fly ash [31] or petroleum pitch with coal fly ash [32]. It can be seen that there are only a limited number of studies on the acid treatment of fly ash followed by carbonization under N_2 atmosphere.

This study evaluates the use of sugarcane bagasse fly ash, a solid waste generated from sugarcane mill boilers, for adsorption of MB. The fly ash was activated by treatment with various acids and simultaneous heating under N_2 atmosphere. The untreated and treated fly ash materials were characterized by N_2 adsorption, thermogravimetric analysis (TGA), pH, pH at the point of zero charge (pH_{pzc}), bulk density, proximate analysis and Fourier transform infrared spectroscopy (FTIR). The untreated and treated fly ash were used as adsorbents for MB removal and the adsorption kinetics and isotherms were investigated. A commercial activated carbon (CAC) was used for comparison. The novelty of this work is the preparation of adsorbents by using low acid concentration combined with conventional heating.

2. Experimental

2.1 Adsorbents

Sugarcane bagasse fly ash (BFA) was collected from a sugar industry located in Northeastern Thailand. The BFA was ground and sieved with mesh no. 40 to get the uniform particle size of 425 µm. Commercial activated carbon (CAC) in powder form was obtained from an activated carbon production company located in Northeastern Thailand, and was used in the dye adsorption experiment without any treatment.

2.2 Fly ash treatment

The sieved BFA was immersed in 1 M HCl, H_2SO_4 or HNO_3 (BFA:acid=1:1 by weight) for 24 h at room temperature. All chemicals were analytical grade (37% for HCl, 98% for H_2SO_4 and 65% for HNO_3) and purchased from ANaPURE. The sample was then washed with distilled water to remove excess acid. The resulting adsorbents were identified with abbreviations according to type of acid as follows: BFA-HCl, BFA-H_2SO_4 and BFA-HNO_3. To improve its porosity, the acid treated fly ash was heated at 900 °C for 1 h under N_2 using a high temperature electric furnace. The N_2 flow was 200 cm^3/min and the heating rate of the furnace was 30 °C/min. The resulting samples are abbreviated as BFA-HCl-N_2, BFA-H_2SO_4-N_2 and BFA-HNO_3-N_2. Finally, the adsorbent with the highest surface area was identified as TFA (treated fly ash) and was selected to study the MB dye adsorption performance.

2.3 Characterization methods

The porosity of the adsorbents was determined by N_2 adsorption at 77 K performed by a porosimeter (ASAP 2460, Micromeritics). The specific surface area (S_{BET}) was then determined from the isotherm using the Brunauer-Emmett-Teller (BET) equation. The Dubinin-Radushkevich (D-R) equation was used to calculate the micropore volume (V_{mic}). The total pore volume (V_T) was estimated at a relative pressure or P/P^o of about 0.99. The mesopore volume (V_{meso}) was calculated by subtraction of the total pore volume with the micropore volume. The average pore size (D_P) was determined using the Barret-Joyner-Halenda (BJH) equation.

Thermal analysis was carried out to determine the thermal stability of the samples. The thermogravimetric analysis (TGA) and differential thermal analysis (DTA) were performed using TG instrument (DTG 60H, Shimadzu) at a heating rate of 10 °C/min from room temperature to 920 °C. The degradation runs were studied under nitrogen and air atmosphere at a flow rate of 60 mL/min.

The pH values of the adsorbents were measured by soaking 2 g of sample in 100 mL of distilled water and the pH was recorded by using pH meter (OHAUS, starter 3100) at 1 h intervals for a period of 24 h [33].

The bulk density was determined by the modified method of Elelu et al. [34]. An empty 10 mL glass graduated cylinder was weighed, filled with the sample, and weighed again. The bulk density was determined by dividing the sample mass by the volume of the measuring cylinder.

Proximate analysis of the samples was performed using standard procedures [35]. The moisture content was determined by drying method according to ASTM D2867. A sample of known mass was placed into the crucible and placed inside an oven (UN, Memmert) at 150 °C for 3 h. The moisture content was calculated from the difference between the sample weight before and after drying divided by the sample weight before drying. The ash content was measured by weighing 1 g sample in a crucible followed by ashing in a muffle furnace at 800 °C for 2 h. The final weight divided by the initial weight is the ash content. Volatile matter content of the adsorbents was determined following ASTM D5832-95. Here, 1 g of adsorbent is weighed in a crucible, covered with a lid, and heated in a furnace at 950 °C for 30 min. All experiments were carried out in triplicate and the average values are reported. Finally, the fixed carbon content is calculated by subtracting the moisture content, ash content and volatile matter from 100%.

The pH at the point of zero charge (pH_{pzc}) was determined by adding 0.1 g of adsorbent to 50 mL solution of 0.01 M NaCl (99% purity, AR grade) with initial pH from 2 to 11 by adjusting with 0.1 M NaOH (98% purity, AR grade) or 0.1 M HCl. The samples were kept for 24 h at room temperature and the final pH was measured [36]. The final pH was plotted versus the initial pH and the pH_{pzc} was obtained from the intersection of this curve with the line that represents pH initial = pH final (line 45°).

Fourier transform infrared (FTIR) spectra of adsorbents were collected using a Tensor 27 (Bruker) in the wavenumber range of 4000-600 cm^{-1} without mixing with KBr. After interpretation of the spectra, the surface functional groups on the adsorbents were obtained.

2.4 Adsorbate

Methylene blue (MB) with a molecular formula of $C_{16}H_{18}N_3SCl$ was chosen as adsorbate in this study. This dye in dark green powder was purchased from QRec. The stock solution of 1000 mg/L was prepared by dissolving 1 g of dye in 1000 mL distilled water. This stock solution was diluted to the desired concentrations that were used in adsorption experiments.

2.5 Adsorption experiments

To investigate the adsorption behavior of the different materials, a series of adsorption experiments was conducted in batch mode to study the adsorption kinetics and adsorption isotherm. All adsorption experiments were carried out in triplicate and the mean values with standard deviation are reported for each test. The residual MB concentration was calculated from a calibration curve by measuring the light absorbance using a UV-vis spectrophotometer (Agilent 8453) at λ_{max}=665 nm. Adsorption kinetics were studied to find out the amount of dye adsorbed at different time points until equilibrium was reached. Experiments were performed using 10 mg/L initial MB concentration (pH=8.46) with 50 mL of solution and 0.05 g adsorbent for 300 min at room temperature. The amount of MB adsorbed onto the adsorbents (q_t, mg/g) at time t was calculated by the following equation:

$$q_t = \frac{V(C_0 - C_t)}{m} \tag{1}$$

where m is the mass of adsorbent (g), V is the volume of MB solution (L), C_o is the initial MB concentration of 10 mg/L and C_t is the MB concentration at time t (mg/L).

In order to investigate the potential rate determining steps for MB adsorption, three kinetic models including pseudo-first order, pseudo-second order and intra-particle diffusion models were used. The pseudo-first order kinetic equation [37] is

$$\frac{dq_t}{dt} = k_1(q_e - q_t) \tag{2}$$

After definite integration by applying the conditions $q_t = 0$ at $t = 0$ and $q_t = q_t$ at $t = t$, the equation becomes:

$$log(q_e - q_t) = logq_e - \frac{k_1 t}{2.303} \tag{3}$$

where q_t is the amount of MB adsorbed (mg/g) at time t (min), q_e is the adsorption capacity at equilibrium (mg/g) and k_1 is the rate constant of pseudo-first order (min^{-1}). The rate constant is determined from the plot of $\log(q_e - q_t)$ against t.

The pseudo-second order kinetic equation [38] is given by

$$\frac{dq_t}{dt} = k_2(q_e - q_t)^2 \tag{4}$$

After integration, the following linear equation is obtained:

$$\frac{t}{q_1} = \frac{1}{k_2 q_e^2} + \frac{t}{q_e} \tag{5}$$

where k_2 is the rate constant (g/mg·min). The q_e and k_2 can be determined from the slope and intercept of plot of t/q_t versus t. The initial adsorption rate, h (mg/g·min), as $t \to 0$ can be defined as

$$h = k_2 {q_e}^2 \tag{6}$$

The value of h was calculated from the intercept of Eqn. (5). The intra-particle diffusion model is given by [38]

$$q_t = k_{id} t^{1/2} + C \tag{7}$$

where k_{id} is the rate constant ($mg/g \cdot min^{1/2}$). A plot of q_t versus $t^{1/2}$ gives a slope k_{id} and intercept C. This model assumes that intra-particle diffusion process is important for the reaction rate [37]. If the adsorption process is mainly controlled by intra-particle diffusion, the intercept of the linear fit is zero. If both internal diffusion and external diffusion influence the adsorption process, the line deviates from the origin.

The effect of the initial concentration on the adsorption behavior was examined by performing adsorption experiments at different concentrations of 10-500 mg/L (pH 8.10-8.38) using the same mass of adsorbent (0.05 g) and the same volume of MB solution (50 mL) at equilibrium time. The MB adsorption capacity of the adsorbents at equilibrium (q_e, mg/g) and the removal efficiency (%Removal) were calculated from Eq. (10) and (11), respectively:

$$q_e = \frac{V(C_0 - C_e)}{m} \tag{8}$$

$$\%Removal = \frac{(C_0 - C_e)}{C_0} \times 100 \tag{9}$$

where C_e is the MB concentration at equilibrium (mg/L).

The equilibrium experimental data obtained for MB adsorption onto the three adsorbents were analyzed using non-linear forms of Langmuir, Freundlich, and Dubinin-Radushkevich (D-R) isotherms given in Eq. (12)-(14), respectively:

$$q_e = \frac{q_m K_L C_e}{(1 + K_L C_e)} \tag{10}$$

$$q_e = K_F C_e{}^{1/n} \tag{11}$$

$$q_e = q_m e^{-K_{DR}\varepsilon^2} \tag{12}$$

where q_e is the adsorbed amount of the MB in mg/g, C_e is the concentration of MB solution at equilibrium in mg/L, q_m is the monolayer adsorption capacity in mg/g, K_L is the Langmuir constant in L/mg, and K_F ((mg/g)·(L/mg)$^{1/n}$) and n are the Freundlich constants. A value of 1/n below 1 indicates a normal Langmuir isotherm while 1/n above 1 is indicate of cooperative adsorption. The 1/n value ranging between 0 and 1 is a measure of adsorption intensity or surface heterogeneity. A 1/n value closer to 0 means a more heterogeneous surface [1]. In Eq. (14), K_{DR} is the coefficient related to the mean free energy of adsorption (mol^2/J^2), and ε is the Polanyi potential:

$$\varepsilon = RTln\left(1 + \frac{1}{C_e}\right) \tag{13}$$

Here, R (the gas constant, 8.314 J/(mol·K) and T is the absolute temperature (303 K). In addition, the D-R model was applied to calculate the mean adsorption energy E (J/mol) [39]:

$$E = \frac{1}{\sqrt{2K_{DR}}} \tag{14}$$

It is noted that due to various effects of linearization, estimation of parameters using regression fit is not a good approach as it leads to spurious correlations [40]. So, this study used the non-linear equations to evaluate the non-linear parameters of the adsorption isotherms. The validity of each model was explained by the correlation coefficient (R^2) and the sum of squared errors or SSE given by [41]:

$$SSE = \sum_{i=1}^{n} (q_{e,model} - q_{e,experiment})^2 \tag{15}$$

A lower values of SSE indicates a better fit. The characteristics of the Langmuir isotherms can be expressed by the dimensionless separation factor (R_L) [42]:

$$R_L = \frac{1}{1 + K_L C_0} \tag{16}$$

where C_0 is the initial MB concentration. There are four possibilities for the R_L value: (1) $0 < R_L < 1$ or favorable adsorption, (2) $R_L > 1$ or unfavorable adsorption, (3) $R_L = 1$ or linear adsorption and (4) $R_L = 0$ or irreversible adsorption. A high value of K_L and low value of R_L indicate a high and favorable solute/adsorbent adsorption process [43].

3. Results and discussion

3.1 Porosities of adsorbents

Figure 1 shows the N_2 adsorption-desorption isotherms for the sugarcane bagasse fly ash (BFA) before and after treatment, as well as the commercial activated carbon (CAC). The untreated BFA shows an initial increase in adsorption at low pressure followed by a flattening of the curve that is typical for an IUPAC Type I profile. This adsorption behavior combined with the large hysteresis loop indicates the presence of both micropores and mesopores (Figure 1 (a)). After treatment, except for the material impregnated with HCl, the N_2 adsorption increases with pressure like a Type IV profile (Figure 1 (b)-(d)), which is likely due to the development of mesopores. The adsorption isotherm of the HCl-treated fly ash shows Type I behavior indicative of micropores (Figure 1 (b)). The CAC has a high N_2 adsorption capacity with Type IV profile typical for both micropores and mesopores (Figure 1 (e)).

The BET surface area (S_{BET}), pore volumes, and average pore diameter (D_P) of the different samples are listed in Table 1. The S_{BET} and total pore volume (V_T) of CAC are higher than that of the bagasse fly ash materials before and after treatment. The acid-treated fly ash samples show a higher surface area and pore volume than the untreated BFA. After further carbonization with N_2, the development of new pores occurs, which increased the surface area and total pore volume. The bagasse fly ash before and after treatment samples show mainly micropores (65-90%) with an average pore size of 2.20-2.98 nm while CAC shows a greater amount of mesopores (96%) with average pore diameter of 3.72 nm.

The maximum S_{BET} of 239 m^2/g (around 9.19 times higher than the starting material BFA) was found for the fly ash treated with HCl followed by carbonization under N_2 (BFA-HCl-N_2). This sample was therefore used as adsorbent to adsorb MB and is abbreviated as TFA (treated fly ash). Table 2 compares the factors of increasing surface area after treatment of fly ash with those reported in literature. It can be seen that the two step treatment used in this study gave a higher increase in surface area than one step treatments [23, 26, 27]. The acid treatment used in this study is also easier than some previous studies, since it was carried out at room temperature without the need for specific equipment such as ultrasonic bath or microwave heating. Our combined treatment method also gave a higher increase than what was found in the preparation of activated carbon from fly ash by using $ZnCl_2$ activation [28].

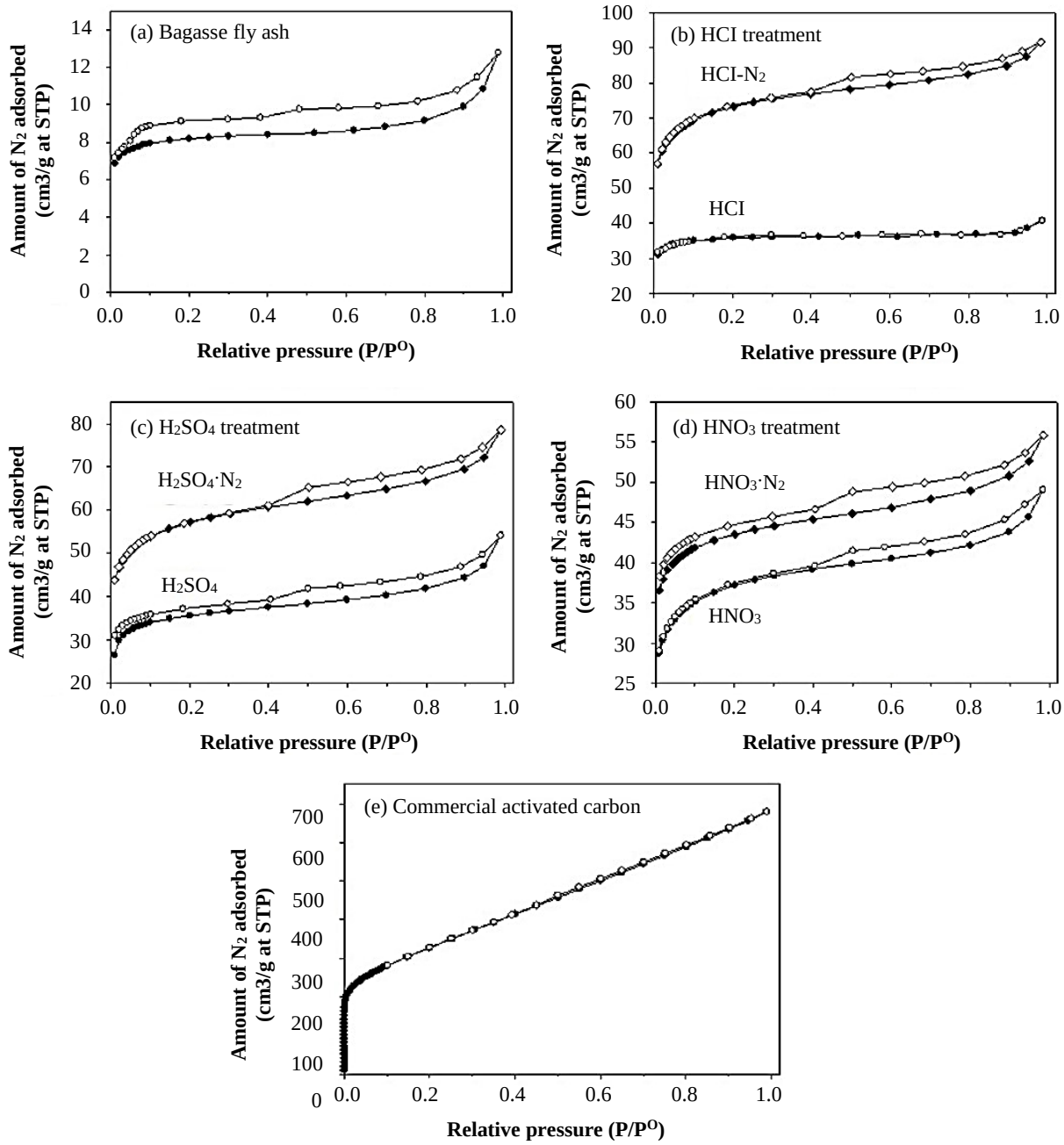

Figure 1 N_2 adsorption-desorption isotherms for (a) bagasse fly ash (BFA), (b) BFA treated with HCl, (c) BFA treated with H_2SO_4, (d) BFA treated with HNO_3 and (e) commercial activated carbon (CAC).

Table 1 Porous properties of bagasse fly ash (BFA) before and after treatment.

Adsorbent	S_{BET} (m^2/g)	V_{mic} (cm^3/g)	V_{meso} (cm^3/g)	V_T (cm^3/g)	D_P (nm)
BFA	26	0.013 (65%)	0.007 (35%)	0.020	2.98
BFA-HCl	114	0.057 (90%)	0.006 (10%)	0.063	2.20
BFA-HCl-N_2 (TFA)	239	0.111 (78%)	0.031 (22%)	0.142	2.37
BFA-H_2SO_4	117	0.058 (69%)	0.026 (31%)	0.084	2.59
BFA-H_2SO_4-N_2	188	0.086 (70%)	0.036 (30%)	0.122	2.87
BFA-HNO_3	122	0.056 (74%)	0.020 (26%)	0.076	2.44
BFA-HNO_3-N_2	142	0.066 (77%)	0.020 (23%)	0.086	2.48
CAC	1130	0.046 (4%)	1.004 (96%)	1.050	3.72

3.2 Characterization of adsorbents used in adsorption study

The thermal stability of the samples measured by thermogravimetric (TG) analysis under N_2 and air atmosphere is shown in Figure 2. In can be seen that the TG curves measured in N_2 atmosphere are shifted to higher temperatures compared to those in air atmosphere. This means that, in order to reach the same weight loss, a higher temperature is required in N_2 atmosphere than in air, indicating thermal decomposition is more efficient in the presence of oxygen. For example, the major weight loss of BFA (Figure 2(a)) is completed at 520 °C in N_2, in contrast to 480 °C in air.

Table 2 Comparison of the factor of increase in surface area by various treatment methods of fly ash.

Treatment method	Factor of increasing S_{BET} compared to untreated fly ash	Reference
1 M HCl at room temperature then carbonized at 900 °C under N_2 for 1 h	9.19	This study
1 M HNO_3 for 24 h	1.76	[26]
3 M NaOH at 100 °C for 72 h	3.41	[23]
3 M NaOH+1.5 M NaCl at 100 °C for 72 h	4.14	[23]
1 M H_2SO_4 for 24 h at 50 °C	3.49	[24]
1 M HCl for 24 h at room temperature	1.81	[27]
1 M HCl at 100 °C for 24 h	1.93	[27]
1 M HCl in an ultrasonic bath for 1 h	1.96	[27]
1 M HCl under microwave heating for 2 and 10 min	1.83-2.29	[27]
Activation with CO_2 at 800 °C for 2 h	1.85	[22]
Concentrated $ZnCl_2$ and then heated at 500-700 °C for 1 h	1.61-3.71	[28]
Concentrated $ZnCl_2$ and then activated with CO_2 at 500-700 °C for 1 h	0.52-3.81	[28]

The TG curves give a clear indication about the thermal degradation behavior. In the first step, the initial weight loss up to 120 °C in both atmospheres was due to water evaporation. Upon further increase of the temperature, a quick weight loss in N_2 atmosphere is observed between 280-520, 500-720 and > 430 °C for BFA, TFA and CAC, respectively. The final weight was 48, 65 and 19 wt% for BFA, TFA and CAC, respectively. These results indicate that TFA had the highest thermal stability. In air atmosphere, the CAC shows the highest weight loss indicating a low ash content. In comparison, both fly ash materials have a low weight loss due to the high ash content.

In both atmospheres, differential thermal analysis (DTA) of all adsorbents presents an endothermic peak between room temperature and 100 °C. The strong exothermic peak is centered between 300-550 °C, 400-720 °C and 300-520 °C for BFA, TFA and CAC, respectively. In air atmosphere, this peak is due to the oxidative degradation of the sample [44] that resulted in the release of CO_2 from the oxidation of unburned carbon [45].

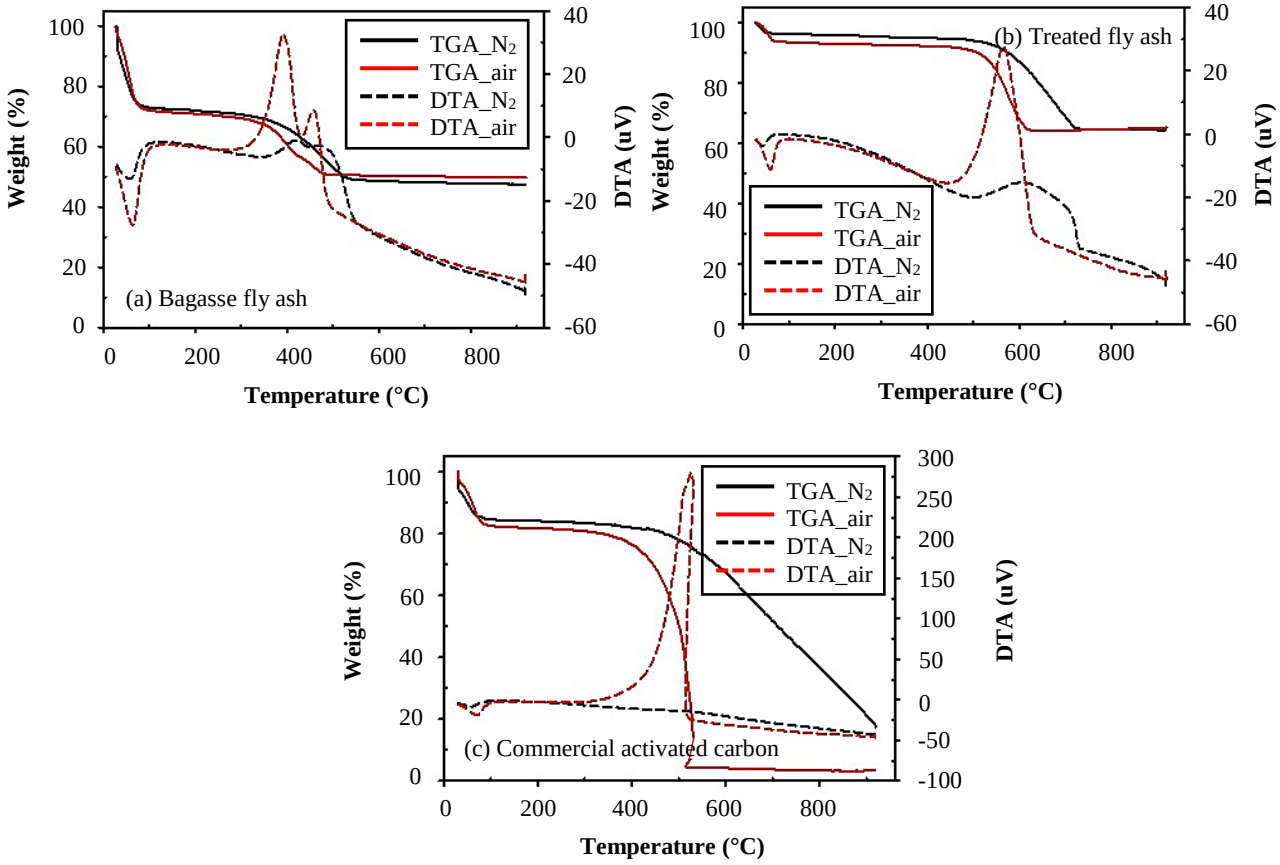

Figure 2 TGA and DTA Plots for all adsorbents.

The physicochemical characteristics of the adsorbents including bagasse fly ash (BFA), bagasse fly ash treated with HCl and N_2 (TFA) and commercial activated carbon (CAC) are presented in Table 3. The pH values of adsorbents were 6.71, 6.85 and 8.37 for BFA, TFA and CAC, respectively. It is noted that the pH of each adsorbent did not significantly change over 24 h, so only the values after 24 h are reported here. For all adsorbents, the pH is close to 7, which is the pH of drinking water, and indicates that these adsorbents can be used to treat water [46].

The amount of adsorbent used is inversely proportional to the bulk density. If the bulk density is high, then the amount of adsorbent needed for a given adsorption capacity will be small [46]. Bulk density depends on the shape, size and density of individual particles and are useful in estimating packing column volume [47]. The bulk density of BFA (0.36 g/cm^3) and TFA (0.38 g/cm^3) did not

significantly differ from each other but were lower than CAC (0.47 g/cm^3). Mall et al. [48] reported a bulk density of 0.133 g/cm^3 for bagasse fly ash while Shah et al. [23] reported a value of 1.74 g/cm^3. This indicated that different cultivation areas and boiler stations gave ashes with a different bulk density.

The moisture content is high for the as-received bagasse fly ash (21.58 wt%). A high moisture content of the adsorbent limits the sample performance and requires an increased adsorbent load. After treatment, the moisture content decreased to 6.93 wt%, which indicates a higher hydrophobicity. The ash content provides information about the inorganic constituents of the sample. This ash content was very high in BFA and TFA in comparison to CAC due to the high minerals content of the fly ash and is in agreement with previous studies [18, 48]. The ash content increased after treatment because the organic compounds in the treated sample decreased while the inorganic compounds content is relatively fixed. Ash content has a significant role in affecting the quality of resulting adsorbent. A high ash content is undesirable since it reduces the adsorption capacity of the adsorbent. Subramanian et al. [49] reported that as-received bagasse fly ash obtained from a sugar mill in Northern India had an ash content of about 80%. The authors separated the carbon-rich fraction by sieving to obtain a particle size of greater than 425 µm, followed by further separation by floating in water. Finally, they prepared activated carbon from separated carbon. However, our study did not separate the carbon fraction due to the purpose of using all parts of solid waste. When compared with BFA, the ash content of TFA increases with a decrease in percentage of volatile matter. It was suggested that acid impregnation and carbonization results in free volatile substance, especially hydrogen, oxygen and nitrogen, that aid in the development of the pore structure [50]. The BFA before and after treatment had a low fixed carbon content while CAC meets the quality standards of activated carbon according to SNI 06-3730-1995 (minimum requirement 60%) [51].

Table 3 Physicochemical characteristics of adsorbents.

	BFA	TFA	CAC
pH	6.71	6.85	8.37
Bulk density (g/cm^3)	0.36	0.38	0.47
Moisture (%)	21.58	6.93	18.45
Volatile matter (%)	27.12	26.60	14.05
Ash (%)	42.46	64.67	4.33
Fixed carbon (%)	8.84	1.80	63.17

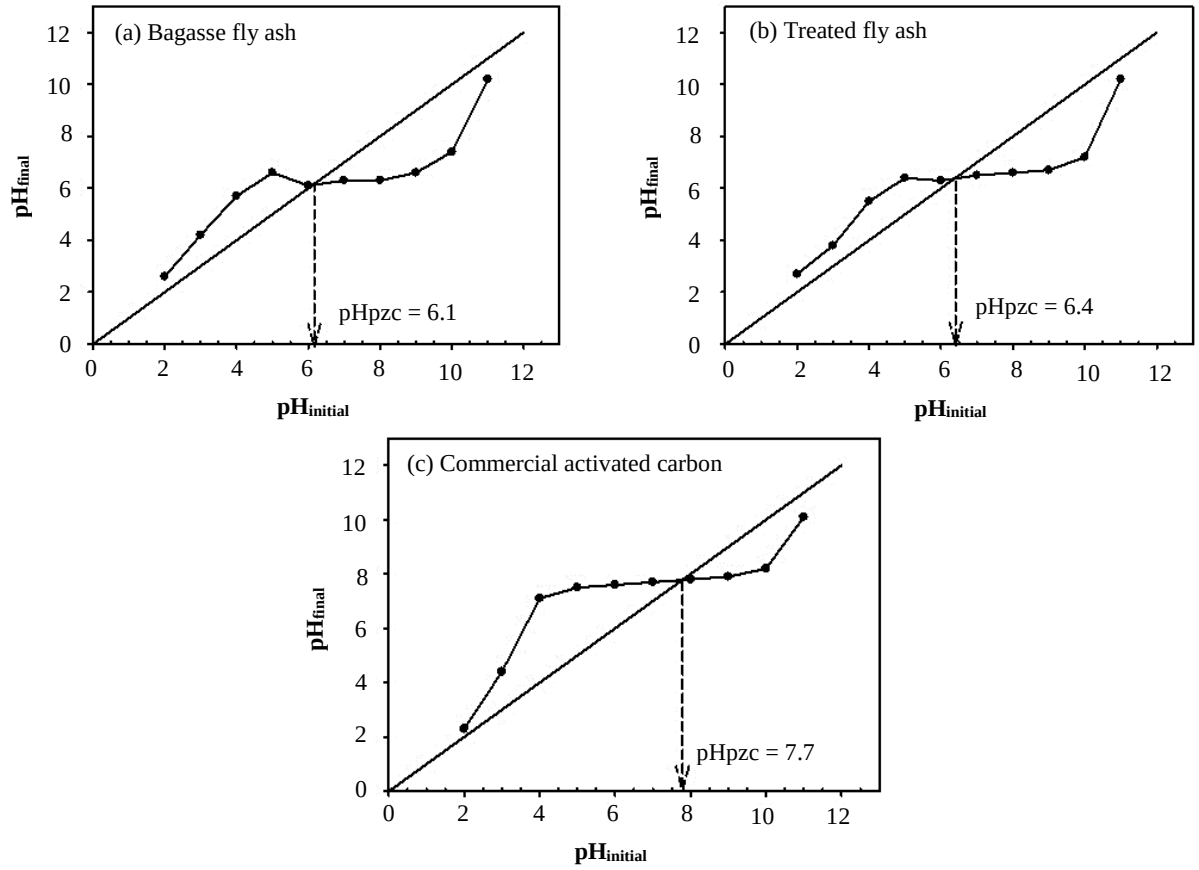

Figure 3 Determination of the pH_{pzc} of the adsorbents.

The pH_{pzc} is an important factor that can provide an indication for the adsorption ability as function of pH [52]. Cationic dye adsorption is favored at pH > pH_{pzc} where the surface becomes negative charged, while anionic dye adsorption is favored at pH < pH_{pzc}. The plot of final pH of adsorbents as a function of its initial pH is given in Figure 3. The pH_{pzc} is 6.1, 6.4 and 7.7 for BFA, TFA and CAC, respectively. These values indicate that both fly ash materials have a slightly acidic character while activated carbon shows a slightly alkaline character. This result is consistent with the pH value of these adsorbents (Table 3).

The FTIR spectra of BFA, TFA and CAC are shown in Figure 4. The broad band between 3600 and 3200 cm^{-1} of BFA corresponds to stretching vibrations of silanol (Si-OH) [23] and other hydroxyl groups as well as adsorbed moisture on the adsorbent surface. The

peak at 1630 cm^{-1} is attributed to hydrogen vibrations, reflecting the presence of bound water, and may also be due to conjugated hydrocarbon bonded carboxyl groups [53]. The treatment of BFA with HCl reduced this peak intensity for TFA, in agreement with the reduced moisture content (Table 3). The presence of the band at 1367 cm^{-1} shows the existence of carboxyl-carbonate structure [54]. The spectra of both BFA and TFA show Si-O-Si bond vibrations at around 1000 cm^{-1} [20, 55] while CAC did not have such peak. A band at 780 cm^{-1} for BFA and 777 cm^{-1} for TFA is due to the presence of Si-C [54]. The CAC has only two weak peaks at 2081 and 1545 cm^{-1} that can be attributed to allene (C=C=C) [56] and aromatic C=C stretching vibrations [28], respectively. The presence of polar groups on the surface of BFA and TFA is likely to give a considerable cation exchange capacity to the adsorbent [57].

Based on the physicochemical characterization, the adsorbents can be divided into 2 different groups. The first group, BFA and TFA, represents adsorbents with low to moderate surface area and pore volume but includes a high density of surface functional groups. In contrast, CAC represents an adsorbent with high surface area and pore volume but has only few functional groups for MB adsorption.

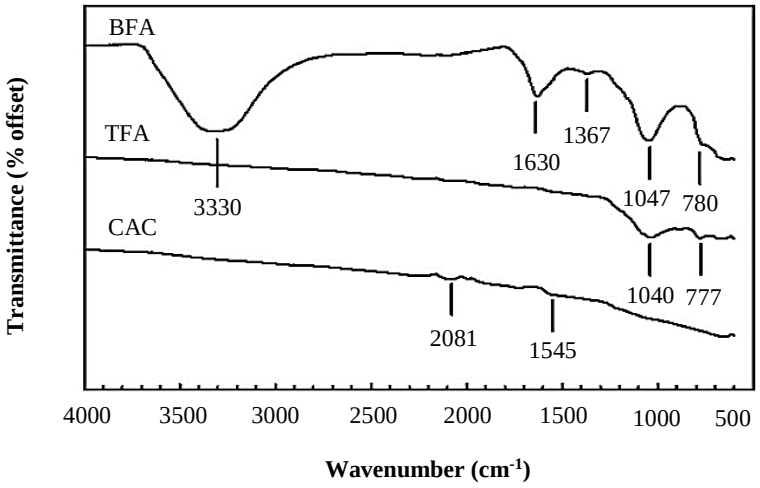

Figure 4 FTIR Spectra of bagasse fly ash (BFA), treated fly ash (TFA), and commercial activated carbon (CAC).

3.3 MB Adsorption kinetics

The effect of contact time on the adsorption capacity of MB for BFA, TFA and CAC is shown in Figure 5. The amount of MB adsorbed significant increased during the first 30 min due to the available vacant surface sites for adsorption. When further increasing the contact time, the adsorption capacity increased slightly and steadily up to 90 min as the active sites become saturated [55]. Thus, 90 min was used as equilibrium time for subsequent experiments.

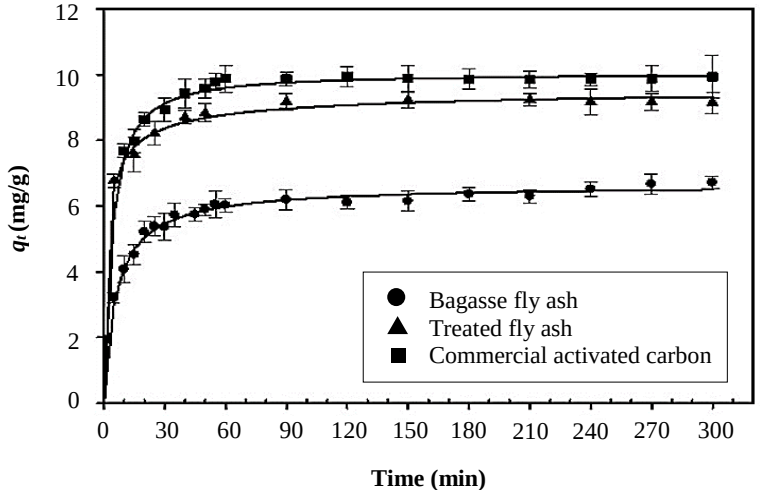

Figure 5 Effect of adsorption time on the removal of MB onto the various adsorbents (initial concentration = 10 mg/L, adsorbent dosage 0.05 g/50 mL MB solution, room temperature).

Three kinetic models (pseudo-first order, pseudo-second order and intra-particle diffusion) were used to describe the MB adsorption behavior. The plots of the linearized forms of the pseudo-first order and pseudo-second order models are shown in Figure 6 and the fitting parameters are summarized in Table 4. The pseudo-second order model gives a better fit of the data compared to the pseudo-first order model. This can also be seen from the low correlation coefficient and a large difference between the experimental and modeled equilibrium adsorption capacity (q_e) for the pseudo-first order model, indicating a poor description of the experimental data. On the contrary, the q_e values obtained from the pseudo-second order equation are very close to the experimental value for all adsorbents. This also confirms the validity of the pseudo-second order kinetic model to the MB adsorption of these adsorbents. The pseudo-second order kinetic model assumes that the adsorption process was chemical adsorption involving electron transfer between adsorbents and adsorbates [37].

The initial adsorption rate (h) was found to be 0.863, 3.958 and 4.283 mg g^{-1} min^{-1} for BFA, TFA and CAC, respectively. This means that the TFA had initial higher adsorption rate than BFA and comparable to CAC. Compared to other studies, the TFA showed a higher initial rate than Cu_2O/TiO_2-CTAB modified geopolymer (0.166-1.2113 mg/g·min) [58], human hair treated with KOH (0.026-0.288 mg/g·min) [59], modified pumice stone with HCl (0.803-1.597 mg/g·min) [60] and fly ash based geopolymer treated with sodium silicate and NaOH (3.779 mg/g·min) [61].

To understand the adsorption mechanism, the kinetic data were further analyzed by the intra-particle diffusion model as shown in Figure 6 (c), and the parameters are presented in Table 4. The intra-particle diffusion model provided a proper fit for all samples. All lines do not pass through the origin, and each line can be separated into two connecting lines with different slopes. This means that not only intra-particle diffusion but both external diffusion and intra-particle diffusion are the rate determining steps for the adsorption of MB on these adsorbents.

The first linear section indicates the initial adsorption stage and reflects the boundary layer thickness [59]. According to Table 4, for all samples the C values increased from the 1st stage to the 2nd stage, which indicated that the boundary layer had a significant influence on the MB adsorption. Thus, the adsorption capacity was exhausted at the 2nd stage and the diffusion became more difficult, resulting in a slower adsorption. This is confirmed by the much smaller k_{id} values for the 2nd stage compared to the 1st stage. Thus, the 1st stage can be attributed to the boundary layer diffusion of dye molecules or external diffusion while the 2nd stage can be attributed to the intra-particle diffusion [62]. Therefore, the adsorption of MB on these adsorbents probably takes place via external adsorption until the active sites are fully occupied (stage 1), after which MB molecules diffuse into the adsorbent pores for further adsorption (stage 2).

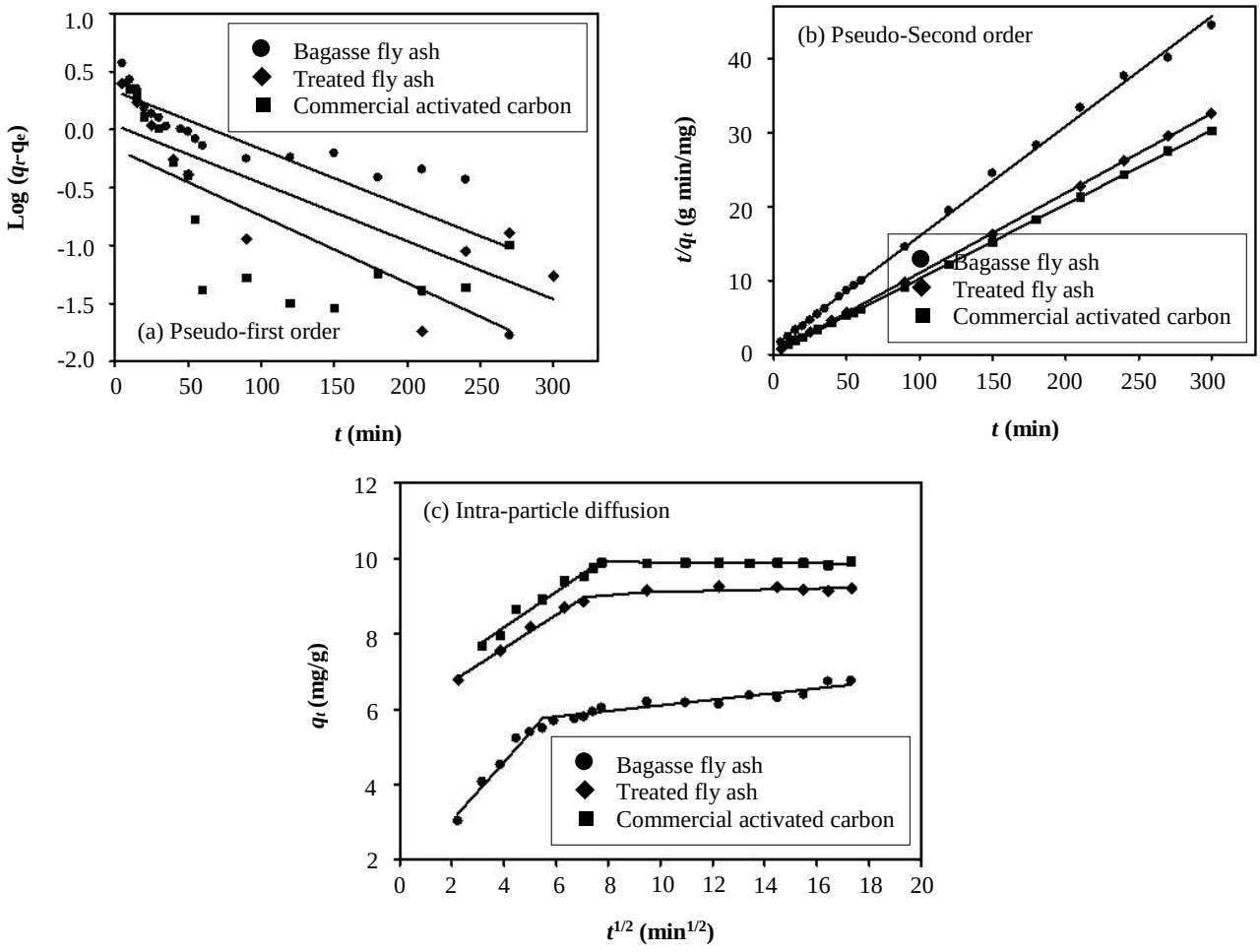

Figure 6 Kinetics plots for MB adsorption on all adsorbents: (a) pseudo-first order model, (b) pseudo-second order model and (c) intra-particle diffusion model.

Table 4 Kinetic parameters for the removal of MB by adsorbents used in this study.

Pseudo-first order				
Adsorbent	**Experimental q_e (mg/g)**	**k_1 (min^{-1})**	**q_e (mg/g)**	**R^2**
BFA	6.751	0.012	2.138	0.720
TFA	9.260	0.012	1.087	0.702
CAC	9.920	0.013	0.684	0.515
Pseudo-second order				
Adsorbent	**Experimental q_e (mg/g)**	**k_2 (g/mg·min)**	**q_e (mg/g)**	**R^2**
BFA	6.751	0.019	6.738	0.998
TFA	9.260	0.046	9.276	0.999
CAC	9.920	0.043	9.980	0.999

Table 4 (continued) Kinetic parameters for the removal of MB by adsorbents used in this study.

Intra-particle diffusion				
Adsorbent		k_{id} **(mg/g·min$^{1/2}$)**	C **(mg/g)**	R^2
BFA	Stage 1	0.775	1.496	0.959
TFA		0.442	5.848	0.987
CAC		0.471	6.283	0.973
BFA	Stage 2	0.075	5.356	0.891
TFA		0.015	8.958	0.875
CAC		0.004	9.931	0.935

3.4 MB Adsorption isotherms

The initial concentration of the dye solution is important because a given mass of adsorbent can adsorb only a fixed amount of adsorbate. Therefore, the effect of initial MB concentration on the removal by BFA, TFA and CAC was studied (Figure 7). In this study, the initial MB solutions had pH values between 8.10-8.38, which are higher than the pH_{pzc} of all adsorbents (6.1 for BFA, 6.4 for TFA, 7.7 for CAC). The surface of adsorbents is negatively charged at pH > pH_{pzc}, therefore, the binding of positively charged MB molecules onto the negatively charged adsorbent surface is facilitated due to electrostatic attraction. So, all adsorbents used in this study were suitable for MB removal.

From Figure 7 (a), it is evident that a high percentage of MB was removed at low initial dye concentrations for all adsorbents. The %Removal decreased on further increase of concentration and the maximum adsorption efficiency (85%) is recorded for TFA. The amount of MB adsorbed per unit mass of adsorbent (Figure 7 (b)) increases with increasing initial dye concentration. This may be due to the decrease in resistance to the uptake of solute from solution of dye [38]. Diagboya and Dikio [63] state that cation movement across the boundary will not be significantly allowed when the transport of cations between the adsorbents' external surface film and internal pores is equal. Increasing the initial MB concentration will stimulate this movement and the amount of dye adsorbed increases.

The uptake of MB on TFA (39 mg/g) increased compared to the untreated BFA (25 mg/g). Despite its lower S_{BET}, the TFA can adsorb MB comparable to the commercial compound (CAC). This indicated that not only surface area and pore volume affect the MB adsorption, but the surface functional group and surface charge are also important. Yuan et al. [64] explained that the cationic MB molecule was adsorbed onto the surface of Si-adsorbent through electrostatic interaction with surface silanol groups (Si-OH). Thus the presence of a large amount of Si-OH for TFA as identified in FTIR spectroscopy may explain the higher MB adsorption capacity onto TFA compared to BFA and CAC. Moreover, since the adsorption energy of the small pores is higher than the large pores, the higher fraction of micropores and smaller average pore size for TFA compared to CAC (Table 1) could explain the comparable adsorption capacity. Since the length of a MB molecule is 1.382 or 1.447 nm and the width is approximately 0.95 nm [41], and the average pore size of TFA is 2.37 nm, the MB molecules can enter the pores of TFA.

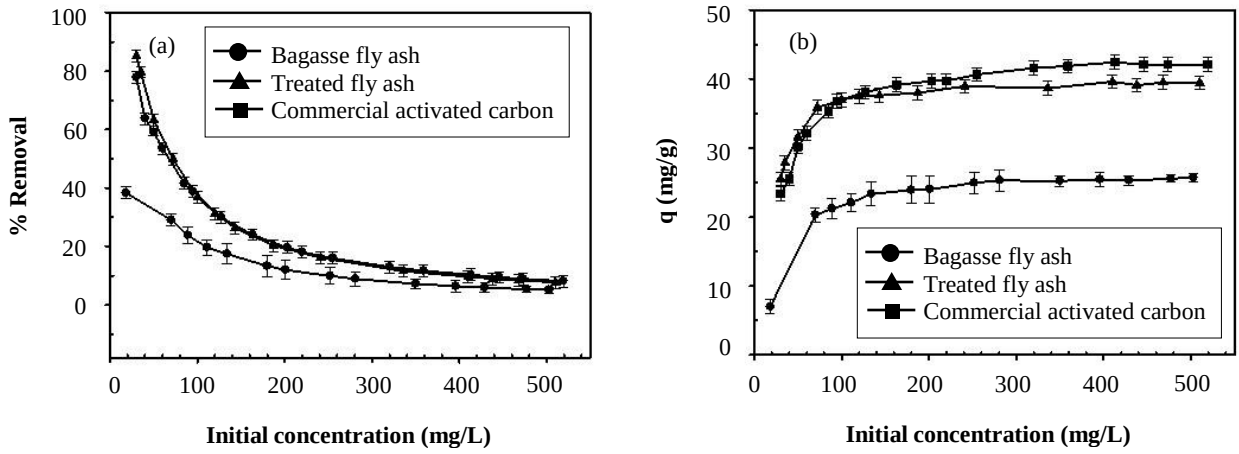

Figure 7 Effect of initial MB concentration on (a) %removal and (b) amount of MB adsorbed onto the various adsorbents (adsorbent dosage 0.05 g/50 mL MB solution, contact time 90 min, room temperature).

The adsorption isotherm is used to investigate how an adsorbate molecule is adsorbed when the adsorbate concentration reaches equilibrium, and also describes the adsorption capacity of the adsorbent [42]. The Langmuir model proposes that adsorption takes place at specific adsorbent sites so that once a dye molecule enters a site no more adsorption can occur at that site when a saturation point (equilibrium) is reached. This is valid for monolayer adsorption onto a surface with a finite number of identical sites. The Langmuir isotherm also assumes that there is no interaction between the molecules adsorbed on neighboring sites [3, 65]. The Freundlich model proposes that adsorption takes place at the interface of heterogeneous surfaces and the adsorption capacity depends on the concentration of molecules at equilibrium. So, this is an isotherm for multilayer adsorption [3, 65].

Figure 8 shows the experimental data (symbols) of C_e and q_e obtained when determining the adsorption capacity of MB onto all three adsorbents. In this figure, the graphs are obtained by fitting the adsorption data to the Langmuir, Freundlich, and D-R models (lines). The better fit to the experimental data obtained by the Langmuir isotherm indicates the homogeneous nature of adsorbents surface and demonstrates the formation of monolayer coverage of dye molecules at the outer surface of the adsorbents [66].

The Langmuir, Freundlich, and D-R constants with the correlation coefficients or R^2 are presented in Table 5. The R^2 values of the Langmuir isotherm are higher than the Freundlich and D-R models, which means that Langmuir isotherm fits the experimental data well. The separation factors (R_L) were in the range of 0-1, indicating that adsorption of MB on all three adsorbents is favorable.

Table 5 also lists the SSE values obtained for the both isotherm models studied. The smaller values of SSE indicate a minimal different between q_e values calculated from the model and the experimental data. The Langmuir isotherm model yields lower SSE values than the Freundlich and D-R isotherm models. This agrees with the higher R^2 values for the Langmuir model and confirms that the adsorption of MB onto all three adsorbents could be best described by the Langmuir isotherm.

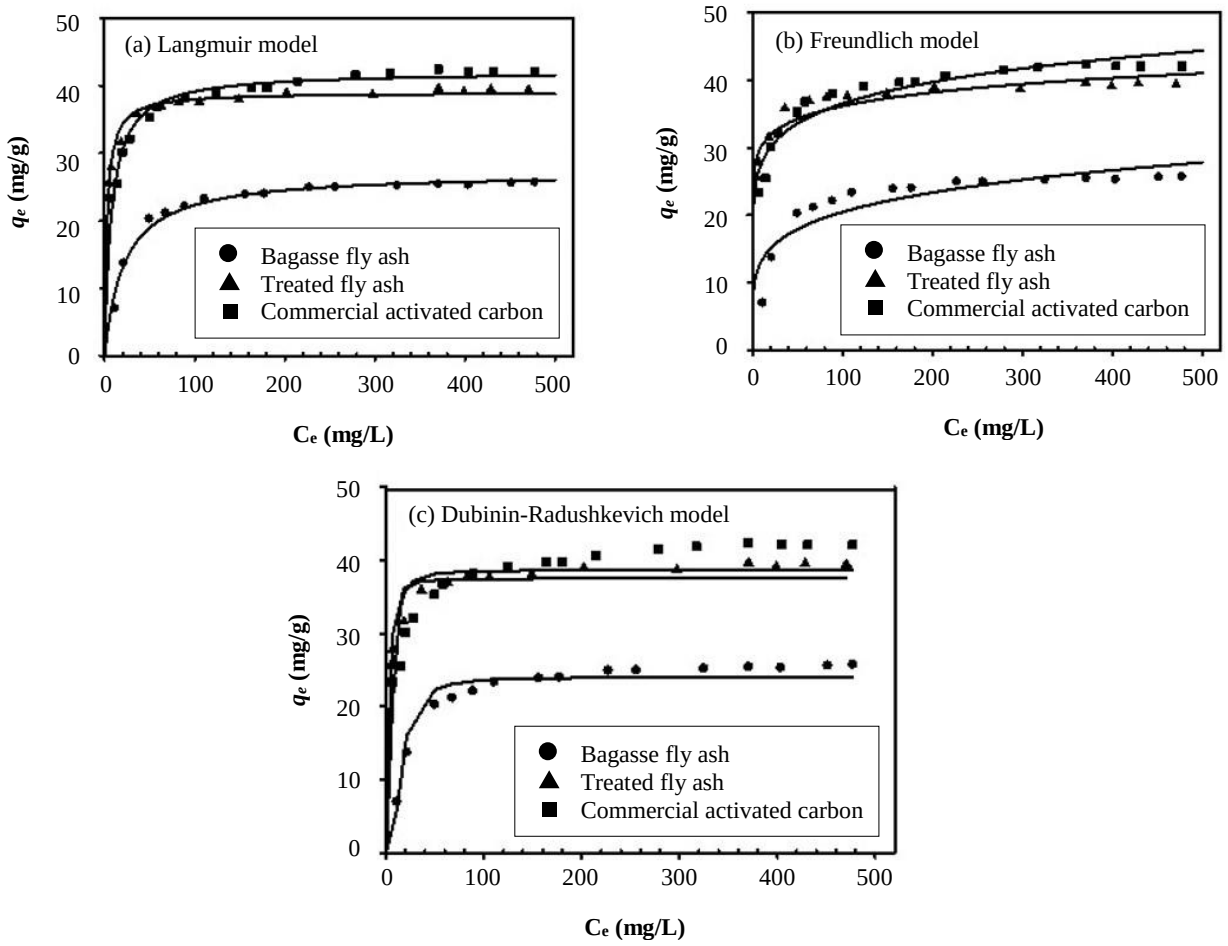

Figure 8 Adsorption isotherm of MB on various adsorbents (a) Langmuir, (b) Freundlich and (c) Dubinin-Radushkevich models.

Table 5 Isotherm parameters for the removal of MB by various adsorbents.

Adsorbent	**Langmuir**				
	q_m **(mg/g)**	K_L **(L/mg)**	R^2	R_L	**SSE**
BFA	27.2	0.046	0.975	0.041–0.543	8.775
TFA	39.0	0.360	0.959	0.005–0.085	10.081
CAC	42.1	0.132	0.951	0.014–0.202	26.572
Adsorbent	**Freundlich**				
	K_F **((mg/g)·(L/mg)$^{1/n}$)**	**1/*n***	***n***	R^2	**SSE**
BFA	8.503	0.191	5.236	0.775	80.045
TFA	25.221	0.078	12.820	0.869	32.373
CAC	20.929	0.121	8.264	0.912	47.711
Adsorbent	**Dubinin-Radushkevich**				
	q_m **(mg/g)**	K_{DR} **(mol^2/J^2)**	***E*** **(J/mol)**	R^2	**SSE**
BFA	24.0	3×10^{-5}	129.1	0.954	28.250
TFA	37.6	2×10^{-6}	500.0	0.806	56.683
CAC	38.6	5×10^{-6}	316.2	0.634	143.980

The adsorption capacity of different adsorbents for MB removal are compared in Table 6. The adsorptive performance of the treated bagasse fly ash (TFA) is higher than or comparable to many adsorbent materials. However, the variation in removal capacity can be attributed to different experimental conditions and physicochemical nature of the adsorbent materials. An advantage of our study over previous work is the simple chemical treatment method without the requirement for specific equipment in the sorbent preparation process. Moreover, the results of this study are in agreement with Aygun et al. [67] who used high surface area granular activated carbons from fruit stones and nutshells (BET surface area 736-793 m^2/g) to adsorb MB and found that the q_m values from Langmuir model were only 1.33-8.82 mg/g. Therefore, not only surface area affects the MB adsorption, but also the surface functional groups and surface charge are determining factors. Previous studies have used raw and treated fly ash as adsorbents for dye removal, but the adsorption capacities are quite low and equilibrium is reached quite slowly. For example, Wang et al. [19] used five coal fly ash to

adsorbed MB and found that maximum adsorption capacity (7 mg/g) was reached after 250 h. Karaca et al. [3] treated coal fly ash with HNO_3 and the maximum MB adsorption capacity was only 0.12 mg/g. Other acid and physical treatments of fly ash also had low MB adsorption capacity of around 0.67-8.00 mg/g [21, 24, 26, 27]. Moreover, the treated fly ash prepared in this study can be applied to treat surface waters due to its neutral pH of 6.85 and by using only a small amount of adsorbent (0.05 g) per 50 mL of wastewater.

Table 6 Comparison of MB adsorption uptake for different adsorbents.

Adsorbents	Adsorption uptake (mg/g)	Reference
Bagasse fly ash treated with HCl and N_2	39.0	This study
Coal fly ash treated with HNO_3	0.1	[3]
Coal fly ash treated with H_2SO_4	0.7	[24]
Almond shell granular activated carbon	1.3	[67]
Fly ash treated with HCl solution in an ultrasonic bath	2.6	[27]
Fly ash treated with HCl solution under microwave heating	2.8	[27]
Mesoporous silica nanoparticles	2.9	[68]
Walnut shell granular activated carbon	3.5	[67]
Apricot stone granular activated carbon	4.1	[67]
Metal-organic frameworks (MOFs) based on copper-benzenetricarboxylates	4.9	[69]
Coal fly ash modified by high-energy ball mill	8.0	[21]
Fly ash treated with HNO_3	8.0	[26]
Hazelnut shell granular activated carbon	8.8	[67]
Nano-silica gel modified by iron and bismuth	9.5	[70]
Magneto-carbon black-clay composite	14.4	[63]
Pumice stone modified with HCl	15.9	[60]
Beech sawdust treated with $CaCl_2$	16.0	[71]
Human hair treated with KOH	17.4	[59]
Leonardite char	26.3	[72]
Fly ash based geopolymer treated with sodium silicate and NaOH	37.0	[61]
Organosolv lignin from rice straw	40.0	[73]
Wood apple rind activated carbon	40.1	[74]

4. Conclusions

Bagasse fly ash (BFA) treated by HCl, H_2SO_4 and HNO_3 followed by carbonization under N_2 atmosphere has been investigated for removal of a cationic dye, methylene blue (MB), from aqueous solution. The combined acid treatment and carbonization greatly improved the surface area and pore volume, and treatment with HCl and N_2 gave the adsorbent with highest specific surface area of 239 m^2/g. The adsorption capacity of this treated fly ash (TFA) sample was compared with untreated BFA and commercial activated carbon. The kinetics study reveals that the adsorption behavior can be described using the pseudo-second order and intra-particle diffusion kinetic models, whereas the adsorption isotherm was best described by the Langmuir model. The maximum MB adsorption capacity of TFA was 39.0 mg/g, which was improved from 27.2 mg/g of the untreated BFA and was comparable to commercial activated carbon (42.1 mg/g) that had a much higher surface area of 1130 m^2/g. This indicated that not only surface area but also surface functional groups and surface charge are main factors that affect the MB adsorption.

5. Acknowledgement

We would like to thank Research and Graduate Studied Division via Sustainable Infrastructure Research and Development Center (SIRDC), Khon Kaen University for research grant.

6. Disclosure statement

No conflict of interest was reported by the authors.

7. References

[1] Hameed BH, Ahmad AL, Latiff KNA. Adsorption of basic dye (methylene blue) onto activated carbon prepared from rattan sawdust. Dyes Pigments. 2007;75(1):143-9.
[2] Mohammed MA, Shitu A, Ibrahim A. Removal of methylene blue using low cost adsorbent: a review. Res J Chem Sci. 2014;4(1):91-102.
[3] Karaca H, Altıntıg E, Turker D, Teker M. An evaluation of coal fly ash as an adsorbent for the removal of methylene blue from aqueous solutions: kinetic and thermodynamic studies. J Dispers Sci Technol. 2018;39(12):1800-7.
[4] Ahmed MJ, Dhedan SK. Equilibrium isotherms and kinetics modeling of methylene blue adsorption on agricultural wastes-based activated carbons. Fluid Phase Equil. 2012;317:9-14.
[5] Cheng J, Zhan C, Wu J, Cui Z, Si J, Wang Q, et al. Highly efficient removal of methylene blue dye from an aqueous solution using cellulose acetate nanofibrous membranes modified by polydopamine. ACS Omega. 2020;5:5389-400.
[6] Zheng L, Su Y, Wang L, Jiang Z. Adsorption and recovery of methylene blue from aqueous solution through ultrafiltration technique. Sep Purif Technol. 2009;68(2):244-9.
[7] Alayli1 A, Nadaroglu H, Turgut E. Nanobiocatalyst beds with Fenton process for removal of methylene blue. Appl Water Sci. 2021;11(2):32.
[8] Dutta K, Mukhopadhyay S, Bhattacharjee S, Chaudhuri B. Chemical oxidation of methylene blue using a Fenton-like reaction. J Hazard Mater. 2001;84(1):57-71.

[9] Contreras M, Grande-Tovar CD, Vallejo WA, Chaves Lopez C. Bio-removal of methylene blue from aqueous solution by Galactomyces geotrichum KL20A. Water. 2019;11(2):282.
[10] Siong VL, Lee KM, Juan JC, Lai CW, Tai XH, Khe CS. Removal of methylene blue dye by solvothermally reduced graphene oxide: a metal-free adsorption and photodegradation method. RSC Adv. 2019;9:37686-95.
[11] El-Ashtoukhy ESZ, Fouad YO. Liquid-liquid extraction of methylene blue dye from aqueous solutions using sodium dodecylbenzenesulfonate as an extractant. Alexandria Eng J. 2015;54(1):77-81.
[12] Liu N, Wu Y. Removal of methylene blue by electrocoagulation: a study of the effect of operational parameters and mechanism. Ionics. 2019;25(8):3953-60.
[13] Pathania D, Sharma S, Singh P. Removal of methylene blue by adsorption onto activated carbon developed from *Ficus carica* bast. Arabian J Chem. 2017;10:S1445-51.
[14] Adesina AO, Elvis OA, Mohallem NDS, Olusegun SJ. Adsorption of methylene blue and congo red from aqueous solution using synthesized alumina-zirconia composite. Environ Technol. 2019;42(7):1061-70.
[15] Wang Y, Pan J, Li YH, Zhang P, Li M, Zheng H, et al. Methylene blue adsorption by activated carbon, nickel alginate/activated carbon aerogel, and nickel alginate/graphene oxide aerogel: a comparison study. J Mater Res Technol. 2020;9(6):12443-60.
[16] Crini G, Lichtfouse E, Wilson LD, Morin-Crini N. Conventional and non-conventional adsorbents for wastewater treatment. Environ Chem Lett. 2019;17(1):195-213.
[17] Santoso E, Ediati R, Kusumawati Y, Bahruji H, Sulistiono DO, Prasetyoko D. Review on recent advances of carbon based adsorbent for methylene blue removal from waste water. Mater Today Chem. 2020;16:100233.
[18] Patel H. Environmental valorization of bagasse fly ash: a review. RSC Adv. 2020;10(52):31611-21.
[19] Wang S, Ma Q, Zhu ZH. Characteristics of coal fly ash and adsorption application. Fuel. 2008;87(15-16):3469-73.
[20] Khan TA, Ali I, Singh VV, Sharma S. Utilization of fly ash as low-cost adsorbent for the removal of methylene blue, malachite green and rhodamine B dyes from textile wastewater. J Environ Protect Sci. 2009;3:11-22.
[21] Li H, Dai M, Dai S, Dong X, Li F. Methylene blue adsorption properties of mechanochemistry modified coal fly ash. Hum Ecol Risk Assess. 2018;24(8):1-9.
[22] Freitas JV, Ruotolo LAM, Farinas CS. Adsorption of inhibitors using a CO_2-activated sugarcane bagasse fly ash for improving enzymatic hydrolysis and alcoholic fermentation in biorefineries. Fuel. 2019;251:1-9.
[23] Shah B, Mistry C, Shah A. Seizure modeling of Pb(II) and Cd(II) from aqueous solution by chemically modified sugarcane bagasse fly ash: isotherms, kinetics, and column study. Environ Sci Pollut Res Int. 2013;20(4):2193-209.
[24] Lin JX, Zhan SL, Fang MH, Qian XQ, Yang H. Adsorption of basic dye from aqueous solution onto fly ash. J Environ Manag. 2008;87(1):193-200.
[25] Jinping L, Jinhua G, Liang W, Juan Y. Preparation of fly ash based adsorbents for removal active red X-3B from dying wastewater. MATEC Web Conf. 2016;67:07004.
[26] Wang S, Boyjoo Y, Choueib A, Zhu ZH. Removal of dyes from aqueous solution using fly ash and red mud. Water Res. 2005;39(1):129-38.
[27] Wang S, Boyjoo Y, Choueib A. A comparative study of dye removal using fly ash treated by different methods. Chemosphere. 2005;60(10):1401-7.
[28] Purnomo CW, Salim C, Hinode H. Preparation and characterization of activated carbon from bagasse fly ash. J Anal Appl Pyrol. 2011;91(1):257-62.
[29] Alhamed YA, Rather SU, El-Shazly AH, Zaman SF, Daous MA, Al-Zahrani AA. Preparation of activated carbon from fly ash and its application for CO_2 capture. Kor J Chem Eng. 2015;32(4):723-30.
[30] Ouyang S, Fu L, Wang Z. Study on activated carbon prepared from coking fly ash with KOH activation. Adv Mater Res. 2012;490-495:3540-4.
[31] Mariana, Mulana F, Djuned FM, Fadli M, Meilian M. Fabrication of activated charcoal from coconut shell combined with coal fly ash from PLTU Nagan Raya for adsorption of methylene blue. IOP Conf Mater Sci Eng. 2020;796:012049.
[32] Kim MI, Im JS, Seo SW, Cho JH, Lee YS, Kim S. Preparation of pitch-based activated carbon with surface-treated fly ash for SO_2 gas removal. Carbon Letter. 2020;30(4):381-7.
[33] Darmayanti L, Notodarmodjo S, Damanhuri E. Removal of copper (II) ions in aqueous solutions by sorption onto fly ash. J Eng Technol Sci. 2017;49(4):546-59.
[34] Elelu SA, Adebayo GB, Abdus-Salom N, Iriowen EM. Preparation and characterization of adsorbents from physic nut plant (*Jatropha Curcas* L.). Chemist. 2018;91(2):42-9.
[35] Kibami D, Pongener C, Rao KS, Sinha D. Preparation and characterization of activated carbon from *Fagopyrum esculentum* Moench by HNO_3 and H_3PO_4 chemical activation. Der Chemica Sinica. 2014:5(4):46-55.
[36] Zhang Z, Moghaddam L, O'Hara IM, Doherty WOS. Congo red adsorption by ball-milled sugarcane bagasse. Chem Eng J. 2011;178:122-8.
[37] Zhou L, Zhou H, Hu Y, Yan S, Yang J. Adsorption removal of cationic dyes from aqueous solutions using ceramic adsorbents prepared from industrial waste coal gangue. J Environ Manag. 2019;234:245-52.
[38] Mall ID, Srivastava VC, Agarwal NK. Removal of orange-g and methyl violet dyes by adsorption onto bagasse fly ash-kinetic study and equilibrium isotherm analyses. Dyes Pigments. 2006;69(3):210-23.
[39] Liu L, Fan S, Li Y. Removal behavior of methylene blue from aqueous solution by tea waste: Kinetics, isotherms and mechanism. Int J Environ Res Public Health. 2018;15(7):1321.
[40] Karri RR, Sahu JN, Jayakumar NS. Optimal isotherm parameters for phenol adsorption from aqueous solutions onto coconut shell based activated carbon: error analysis of linear and non-linear methods. J Taiwan Inst Chem Eng. 2017;80:472-87.
[41] Jia P, Tan H, Liu K, Gao W. Removal of methylene blue from aqueous solution by bone char. Appl Sci. 2018;8(10):1903.
[42] Rai P, Gautam RK, Banerjee S, Rawat V, Chattoapadhyaya MC. Synthesis and characterization of a novel $SnFe_2O_4$@activated carbon magnetic nanocomposite and its effectiveness in the removal of crystal violet from aqueous solution. J Environ Chem Eng. 2015;3(4):2281-91.
[43] Ahmad F, Daud WM, Ahmad MA, Radzi R. Cocoa (*Theobroma cacao*) shell-based activated carbon by CO_2 activation in removing of cationic dye from aqueous solution: kinetics and equilibrium studies. Chem Eng Res Des. 2012;90(10):1480-90.
[44] Suresh S. Adsorption of benzoic acid in aqueous solution by bagasse fly ash. J Inst Eng India Ser A. 2012;93(3):151-61.

[45] Mohebbi M, Rajabipour F, Scheetz BE. Evaluation of two-atmosphere thermogravimetric analysis for determining the unburned carbon content in fly ash. Adv Civ Eng Mater. 2017;6(1):258-79.
[46] Christian NS, Manga NH, Raoul TTD, Gabche AS. Optimisation of activated carbon preparation by chemical activation of *Ayous* Sawdust, *Cucurbitaceae* peelings and hen egg shells using response surface methodology. Int Res J Pure Appl Chem. 2017;14(4):1-12.
[47] Razi MAM, Suraya WMSW, Rafidah H, Amirza ARM, Attahirah MHMN, Hani MSNQ, et al. Effect of phosphoric acid concentration on the characteristics of sugarcane bagasse activated carbon. IOP Conf Mater Sci Eng. 2015;136(1):012061.
[48] Mall ID, Srivastava VC, Agarwal NK, Mishra IM. Removal of congo red from aqueous solution by bagasse fly ash and activated carbon: kinetic study and equilibrium isotherm analyses. Chemosphere. 2005;61(4):492-501.
[49] Subramanian S, Pande G, Weireld GD, Giraudon JM, Lamonier JF, Batra VS. Sugarcane bagasse fly ash as an attractive agro-industry source for VOC removal on porous carbon. Ind Crops Prod. 2013;49:108-16.
[50] Rodriguez-Reinoso F, Silvestre-Albero J. Activated carbon and adsorption. Reference Module in Materials Science and Materials Engineering. Amsterdam: Elsevier; 2016.
[51] Maulina S, Iriansyah M. Characteristics of activated carbon resulted from pyrolysis of the oil palm fronds powder. IOP Conf Mater Sci Eng. 2018;309(1):012072.
[52] Chham A, Khouya EH, Oumam M, Abourriche A, Gmouh S. Iarzek M, et al. The use of insoluble mater of Moroccan oil shale for removal of dyes from aqueous solution. Chem Int. 2018;4(1):67-77.
[53] Lataye DH, Mishra IM, Mall ID. Removal of pyridine from aqueous solution by adsorption on bagasse fly ash. Ind Eng Chem Res. 2006;45(11):3934-43.
[54] Verma S, Prasad B, Mishra IM. Treatment of purified terephthalic acid wastewater using a bio-waste-adsorbent bagasse fly ash (BFA). Environ Sci Pollut Res Int. 2017;24(2):1953-66.
[55] Zanele ZP, Mtunzi FM, Nelana SM, Ebelegi AN, Ayawei N, Dikio ED, et al. Metals and antibiotics as aqueous sequestration targets for magnetic polyamidoamine-grafted SBA-15. Langmuir. 2021;37:9764-73.
[56] Islam MS, Ang BC, Gharehkhani S, Afif ABM. Adsorption capability of activated carbon synthesized from coconut shell. Carbon Letter. 2016;20(1):1-9.
[57] Mall ID, Srivastava VC, Agarwal NK, Mishra IM. Adsorptive removal of malachite green dye from aqueous solution by bagasse fly ash and activated carbon-kinetic study and equilibrium isotherm analyses. Colloids Surf A Physicochem Eng Asp. 2005;264(1-3):17-28.
[58] Falah M, MacKenzie KJD, Knibbe R, Page SJ, Hanna JV. New composites of nanoparticle Cu (I) oxide and titania in a novel inorganic polymer (geopolymer) matrix for destruction of dyes and hazardous organic pollutants. J Hazard Mater. 2016;318:772-82.
[59] Ahmad Zaini MA, Sudi RM. Valorization of human hair as methylene blue dye adsorbents. Green Process Synth. 2018;7(4):344-52.
[60] Derakhshan Z, Baghapour MA, Ranjbar M, Faramarzian M. Adsorption of methylene blue dye from aqueous solutions by modified pumice stone: kinetics and Equilibrium studies. Health Scope. 2013;2(3):136-44.
[61] El Alouani M, Alehyen S, El Achouri M, Taibi M. Comparative studies on removal of textile dye into geopolymeric adsorbents. Environ Asia. 2019;12(1):143-53.
[62] Liu QX, Zhou YR, Wang M, Zhang Q, Ji T, Chen, TY, et al. Adsorption of methylene blue from aqueous solution onto visco-based activated carbon fiber felts: kinetics and equilibrium studies. Adsorp Sci Technol. 2019;37:312-32.
[63] Diagboya PN, Dikio ED. Scavenging of aqueous toxic organic and inorganic cations using novel facile magneto-carbon black-clay composite adsorbent. J Clean Prod. 2018;180:71-80.
[64] Yuan N, Cai H, Liu T, Huang Q, Zhang X. Adsorptive removal of methylene blue from aqueous solution using coal fly ash-derived mesoporous silica material. Adsorp Sci Technol. 2019;37(4):333-48.
[65] Belhachemi M, Addoun F. Comparative adsorption isotherms and modeling of methylene blue onto activated carbons. Appl Water Sci. 2011;1(3):111-7.
[66] Bagci S, Ceyhan AA. Adsorption of methylene blue onto activated carbon prepared from *Lupinus albus*. Chem Ind Chem Eng Q. 2015;22(2):155-65.
[67] Aygun A, Yenisoy-Karakaş S, Duman I. Production of granular activated carbon from fruit stones and nutshells and evaluation of their physical, chemical and adsorption properties. Microporous Mesoporous Mater. 2003;66(2-3):189-95.
[68] Chueachot R, Wongkhueng S, Khankam K, Lakrathok A, Kaewnon T, Naowanon WT, et al. Adsorption efficiency of methylene blue from aqueous solution with amine-functionalized mesoporous silica nanospheres by co-condensation biphasic synthesis: adsorption condition and equilibrium studies. Mater Today Proc. 2018;5(6):14079-85.
[69] Lin S, Song Z, Che G, Ren A, Li P, Liu C, et al. Adsorption behavior of metal-organic frameworks for methylene blue from aqueous solution. Microporous Mesoporous Mater. 2014;193:27-34.
[70] Salimi F, Tahmasobi K, Karami C, Jahangiri A. Preparation of modified nano-SiO_2 by bismuth and iron as a novel remover of methylene blue from water solution. J Mex Chem Soc. 2017;61(3):250-9.
[71] Batzias FA, Sidiras DK. Dye adsorption by calcium chloride treated beech sawdust in batch and fixed-bed systems. J Hazard Mater. 2004;114(1-3):167-74.
[72] Hemaviboon K, Klamtet J. Removal of methylene blue dye from aqueous solution by adsorption on leonardite char. Naresuan Uni J Sci Tech. 2020;28(1):82-93.
[73] Zhang S, Wang Z, Zhang Y, Pan H, Tao L. Adsorption of methylene blue on organosolv lignin from rice straw. Procedia Environ Sci. 2016;31:3-11.
[74] Malarvizhi R, Ho YS. The influence of pH and the structure of the dye molecules on adsorption isotherm modeling using activated carbon. Desalination. 2010;264(1-2):97-101.